



Eidgenössische Technische Hochschule Zürich  
Swiss Federal Institute of Technology Zurich

SEMESTER THESIS

---

# Calibration of an IQ mixer for continuous and pulsed modulation

---

*Author:*

ANTONIO RUBIO ABADAL

*Supervisor:*

SIMON BERGER

*Professor:*

Prof. ANDREAS WALLRAFF

Quantum Device Lab  
Laboratory for Solid State Physics  
Eidgenössische Technische Hochschule Zürich

August 2014



# Abstract

The experiments routinely performed in circuit quantum electrodynamics (circuit QED) require time-resolved manipulation of the superconducting qubits. This requirement implies that the frequency, amplitude and phase of a microwave carrier signal must be accurately controlled. IQ (In-phase/Quadrature) microwave mixers offer a suitable way to modulate such signals. In this semester thesis, an IQ mixer used for the upconversion of microwave signals is calibrated to minimize the leakage of the local oscillator input signal and to perform single sideband modulation. Some properties and imperfections of the mixer are studied by applying continuous waves to its ports. To avoid an unwanted driving of the resonator and the qubit, nano-second pulsed signals are also generated and sent to the mixer, and the performance of the device analysed in such conditions.



# Contents

<b>1</b>	<b>Motivation</b>	<b>1</b>
<b>2</b>	<b>Mixer theory</b>	<b>2</b>
2.1	The microwave mixer . . . . .	2
2.2	Imperfections of a microwave mixer . . . . .	3
2.2.1	Ideal single diode mixer model . . . . .	3
2.2.2	Realistic single diode mixer . . . . .	3
2.2.3	Nonlinear operation of the mixer . . . . .	4
2.3	IQ mixers . . . . .	5
2.3.1	Direct modulation . . . . .	6
2.3.2	Single sideband upconversion . . . . .	7
2.3.3	Imperfections of IQ mixers . . . . .	7
<b>3</b>	<b>Experimental procedure</b>	<b>9</b>
3.1	The experimental setup . . . . .	9
3.1.1	The IQ microwave mixer . . . . .	9
3.1.2	The upconversion box . . . . .	10
3.1.3	The downconversion box . . . . .	11
3.1.4	Configuration of the AWG . . . . .	11
3.2	IQ mixer calibration for continuous waves . . . . .	12
3.2.1	DC-offset calibration . . . . .	12
3.2.2	Sideband calibration . . . . .	13
3.3	Pulsed direct modulation . . . . .	13
<b>4</b>	<b>Results of the calibration</b>	<b>15</b>
4.1	Spectrum with continuous wave single sideband calibration . . . . .	15
4.2	Nonlinearity of the mixer . . . . .	16
4.3	Direct pulsed modulation . . . . .	18
<b>5</b>	<b>Conclusions</b>	<b>21</b>
	<b>Bibliography</b>	<b>22</b>

# Chapter 1

## Motivation

Among the DiVincenzo criteria for the physical realization of quantum computation, the ability to initialize the state of the qubit, manipulate it –through the application of quantum gates– and perform read-out on the qubit state are fundamental requirements and particularly challenging, as they still require strong isolation from the environment while allowing to address the qubits [1]. When performing experiments with superconducting qubits, and in particular in circuit quantum electrodynamics (circuit QED), the manipulation and measurement of the state of the qubits is done by applying microwave frequency fields to a resonator, which couples to the transmon qubit [2]. The dispersive readout of the state of the qubit also requires a precise measurement of the phase and amplitude of microwave fields transmitted through the resonator [3, 4]. Because of these requirements, the generation of microwave fields with precise control over their frequency, amplitude and phase is an essential task. To do so, it is frequently necessary to translate the frequencies of these fields between the ones at which the microwave instruments work and the ones relevant for the circuit QED sample. The main tool for such tasks is a microwave frequency mixer.

Though for an ideal frequency mixer it would be possible to have a signal with a single frequency at the output port, real mixers present imperfections which cause signal leakage as well as the generation of signals at unwanted frequencies [5]. Calibrating the mixer can yield a strong cancellation of these imperfections, which is an essential step for the precise control of the qubits. In the particular case of the study of geometric phases in superconducting qubits [6], these additional frequencies have to be carefully considered, as the state of the qubits is specially sensitive to signals at such close frequencies. Because of this fact, it is frequently desired to work with really short pulses (nano-second) of microwave fields in this kind of experiments, as this procedure avoids the unwanted driving of the system. In this semester thesis an IQ (In-phase/Quadrature) mixer will be calibrated for the modulation of both continuous and pulsed microwave fields, and its performance in different conditions studied.

# Chapter 2

## Mixer theory

As it has been emphasized in the motivation chapter, microwave frequency mixers constitute one of the basic elements for the manipulation and read-out of superconducting qubits. In this chapter the properties, imperfections and metrics of microwave mixers are described, as the knowledge of these different aspects will be necessary to understand the contents of the following chapters. IQ mixers are also explained and how they can be used to perform direct and single sideband modulation.

### 2.1 The microwave mixer

Frequency mixers are nonlinear electrical circuits which are able to output an electromagnetic signal with a different frequency from the input signal applied to it. Standard mixers have 3 ports. The names of these 3 mixer ports are the Local Oscillator (LO) port, the Radio Frequency (RF) port and the Intermediate Frequency (IF) port. The LO port is usually used as an input port, while the RF and the IF ports can either be the second input or the output of the mixer –this depends on the application of the mixer.

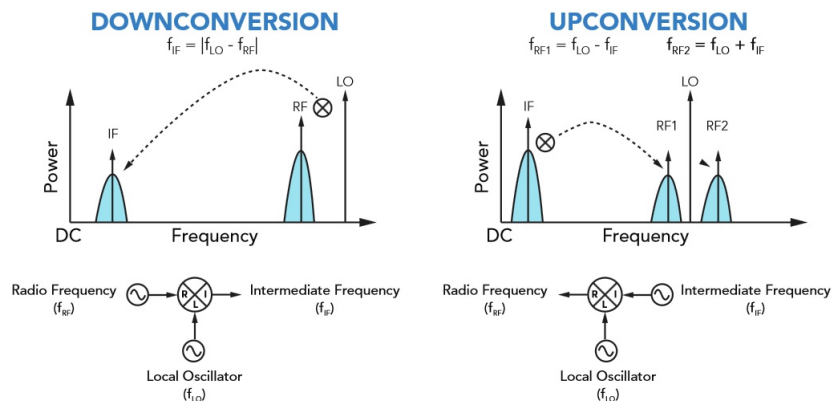


FIGURE 2.1: Description of the processes of downconversion and upconversion. Figure taken from [5].

In the ideal case, a mixer gives an output frequency which is either the sum or the difference of the two inputs frequencies. When an output signal with higher frequency than the one in the second input is desired, the IF is used as the input and the RF as the output, in a process called upconversion. If the desired output frequency is lower than the second input, the RF becomes the input and the IF the output, in what we call downconversion. So in the case of upconversion there will be two main mixing products (signal with frequencies  $f_{RF1} = f_{LO} - f_{IF}$  and  $f_{RF2} = f_{LO} + f_{IF}$ ) while in the case of downconversion there is a single-frequency signal as main product (with  $f_{IF} = |f_{LO} - f_{RF}|$ ). Both of these processes are described in figure 2.1.

To perform their functionality, mixers use a technique called heterodyning, which is exactly the process which generates signals with new frequencies (heterodynes) from the ones in the input. To build a mixer and be able to do this heterodyning technique, the main ingredient that is needed is a nonlinear device. The main devices used for designing microwave mixers are Schottky diodes, GaAs FETs and CMOS transistors [5]. All the microwave mixers used in this project are designed using Schottky diodes, so we will only focus on describing the details of this kind of mixers.

## 2.2 Imperfections of a microwave mixer

In this section it will be shown how some properties of an “ideal mixer” are not totally fulfilled in the real case. To illustrate this situation, we will assume the simplest kind of mixer, which would be built with a single diode. We will also consider in this section, only to simplify the notation, that the RF port is used for the input signal and the IF for the output.

### 2.2.1 Ideal single diode mixer model

The structure of the single diode mixer circuit is the one shown in figure 2.2(a), where the mixer is also supposed to be single-ended. We continue by considering a couple of assumptions on the used diode. The first one is that it behaves like an ideal commutator, so that it switches immediately. This immediate switch is implied in the relation between current and voltage in figure 2.2(b). The second is that the LO signal is the only one that affects the transconductance of the diode, as it is assumed to be much stronger than the RF signal ( $P_{LO} \gg P_{RF}$ ).

In the output IF signal a “chopped” RF signal will be produced, as the signal will only be transmitted when the diode is not switched. As the switching depends only on the LO signal, the “chopping” will have the frequency of the LO. In this conditions, the only possible mixing output products will be signals which obey the relation  $f_{IF} = n f_{LO} \pm f_{RF}$ , where  $n$  is an odd integer [5]. This behaviour is shown in the first graphic of figure 2.3.

### 2.2.2 Realistic single diode mixer

In the real situation, the diode does not behave like an ideal commutator, but it rather has a region where it is turned on. This behaviour is shown by the Shockley diode



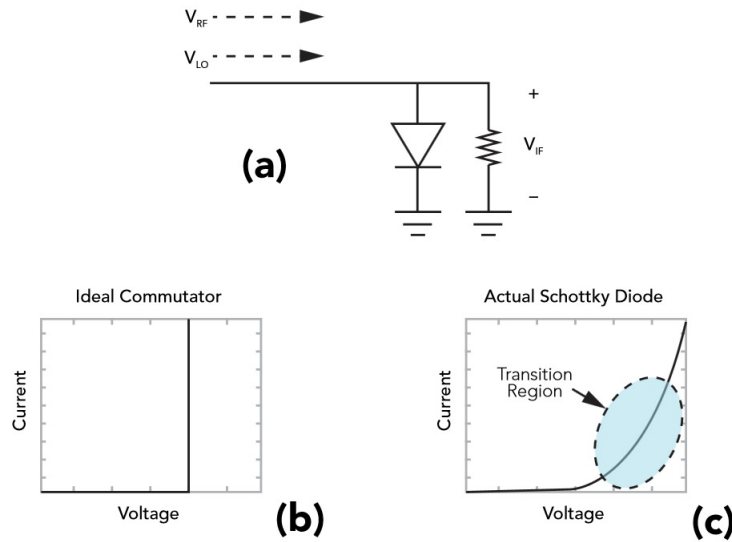


FIGURE 2.2: (a) Structure of a single-ended single diode mixer. (b) Current and voltage relation for an ideal commutator. (c) Realistic Schottky Diode current and voltage relation, with the transition region shadowed. Figure taken from [5].

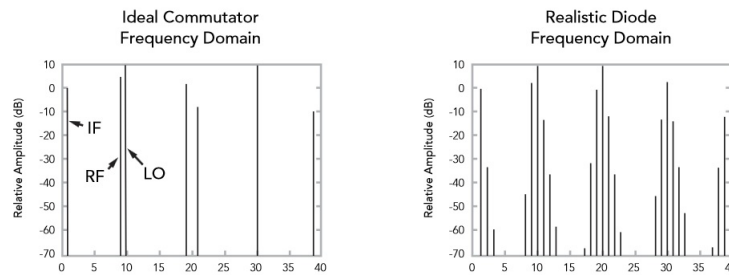


FIGURE 2.3: Graphics corresponding to the frequency domain of a mixer with an ideal commutator and with a mixer with a realistic diode. Figure taken from [5].

equation and is represented in the current-voltage graphic of figure 2.2(c). Furthermore, the RF signal will also affect the transconductance of the diode to some extent, specially when the input power in the RF gets higher. The main consequence of this nonideality is that additional mixing products will be obtained aside from the ones described just below [5]. Every harmonic combination can be obtained in the output, so the signals will instead obey the relation  $f_{IF} = nf_{LO} \pm mf_{RF}$ , where  $m$  and  $n$  are integers. The corresponding frequency domain is shown in the second graphic of figure 2.3. In our experiments we will be only interested in having a single frequency product, so obviously these nonidealities will be an important problem to be taken into account.

### 2.2.3 Nonlinear operation of the mixer

When the input RF power grows, it also has some consequences in the relation between the input and output power of the mixer. To understand this situation, it is important first to define the conversion loss of the mixer.

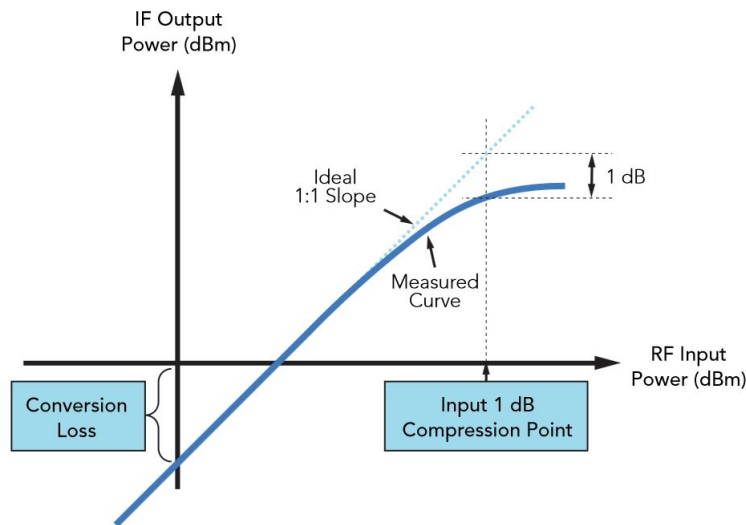


FIGURE 2.4: Representation of the mixer non-linearity and the 1 dB compression point. Figure taken from [5].

The conversion loss is the most important metric of a microwave mixer. It is a measure of how efficiently the mixer shifts the frequency of the RF signal to the IF signal. It is measured in dB and it can be expressed as

$$CL = 10 \log_{10} \left( \frac{P_{RF}}{P_{IF}} \right) \quad (2.1)$$

or if we represent the power in logarithmic units (e.g. dBm)

$$CL = P_{RF} - P_{IF}. \quad (2.2)$$

This conversion loss is usually constant for small values of the input power in the RF port. This means that an increase of 1 dBm in the input RF power will make the output IF power increase by also 1 dBm. However, if the applied power in the RF signal gets too large, the mixer will start deviating from this linear behaviour and it will begin to saturate, as it is shown in figure 2.4, therefore increasing the conversion loss. This is what we call the mixer compression, and it is used to define the 1 dB compression point, which is a very important characteristic of a mixer. It is defined as the input RF power at which the conversion loss has increased in 1 dB respect to its linear value. This compression occurs when the power of the RF signal cannot be considered much smaller than the power of the LO signal, therefore competing with this one in the switching action of the diode. The operation of the mixer at such signal powers is something we will want to avoid, therefore we must know at which powers will we find this behaviour.

## 2.3 IQ mixers

Aside from the three-port mixers described in the previous section, it is possible to build other kinds of mixers, in most cases built with three-port mixers as basic components.

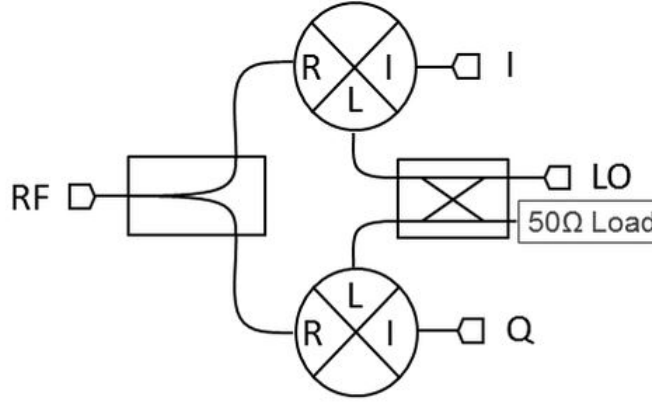


FIGURE 2.5: Internal structure of an IQ mixer. Figure taken from [8].

The most important example to be commented in the context of this thesis is the IQ mixer, also called quadrature IF mixer [7], as it is also the only kind of mixer used in our experimental setup. IQ mixers are used in telecommunications to maximize the information transmission in a limited bandwidth by using quadrature modulation. Quadrature modulation means that both the in-phase and quadrature components of a signal can be modulated. Because of this property, they can be used to control precisely the amplitude and phase of the output signal, a functionality clearly desirable, but they also have the great advantage of allowing to be used as a Single Sideband (SSB) mixers.

The structure of an IQ mixer can be understood by observing figure 2.5. It is built out of two regular mixers and a quadrature hybrid coupler in the LO. The hybrid coupler splits the signal of the LO into two output ports, with a phase shift of  $90^\circ$  in one of them. In upconversion, each of these outputs is either mixed with the In-phase signal or the Quadrature signal and then both outputs are combined in the RF port. On the other hand, if the mixer is used for downconversion it will allow to retrieve both I and Q original data signals in the RF input.

### 2.3.1 Direct modulation

To understand how the amplitude and phase of the output signal can be controlled with an IQ mixer by performing direct modulation, it is convenient to write down the output waveform of the mixer. If we consider a continuous wave in the LO input as  $L(t) = A_{LO} \cos(\omega_{LO}t)$ , then we will get in the output of the hybrid coupler the signals  $L_I(t) = A \cos(\omega_{LO}t)$  and  $L_Q(t) = A \sin(\omega_{LO}t)$ . If we apply a DC voltage in both I and Q, the output signal in the RF will be  $s_{RF}(t) = V_I \cos(\omega_{LO}t) + V_Q \sin(\omega_{LO}t)$ , which can also be rewritten as  $s_{RF}(t) = A_{RF} \cos(\omega_{LO}t + \phi)$ , where  $A_{RF}$  and  $\phi$  are defined by

$$A_{RF} = \sqrt{V_I^2 + V_Q^2} \quad \text{and} \quad \phi = \arctan\left(\frac{V_I}{V_Q}\right) \quad (2.3)$$

Therefore it is clear that by modulating the DC input voltage in both I and Q we can control the amplitude and phase of the output wave in the RF.

### 2.3.2 Single sideband upconversion

Even though applying a DC voltage in the I and Q ports allows us to control the amplitude and phase of our carrier signal, it is important to notice that this carrier signal is at the same frequency as the LO signal. There are several reasons why we would prefer to avoid a carrier signal at this particular frequency, the main one being that mixers show a certain leakage of the LO signal to the RF port, which means that even if we do not apply any voltage in the I and Q ports we will still get a certain drive at the qubit frequency. For this reason, in most situations we will be interested instead in performing single sideband upconversion by applying oscillating signals in the I and Q ports.

If we apply to the I and Q ports the waveforms

$$\begin{aligned} s_I(t) &= I \cos(\omega_{IF}t + \phi_I) \\ s_Q(t) &= Q \cos(\omega_{IF}t + \phi_Q), \end{aligned} \quad (2.4)$$

by the previous expression we see that the RF output will result

$$\begin{aligned} s_{RF} &= \frac{1}{2} [I \cos(\omega_{LO}t) \cos(\omega_{IF}t + \phi_I) + Q \sin(\omega_{LO}t) \cos(\omega_{IF}t + \phi_Q)] \\ &= \frac{1}{4} I [\cos((\omega_{LO} + \omega_{IF})t + \phi_I) + \cos((\omega_{LO} - \omega_{IF})t - \phi_I)] \\ &\quad + \frac{1}{4} Q [\sin((\omega_{LO} + \omega_{IF})t + \phi_Q) + \sin((\omega_{LO} - \omega_{IF})t - \phi_Q)]. \end{aligned} \quad (2.5)$$

From this last expression we see that we have two signals at frequencies  $\omega_{LO} + \omega_{IF}$  and  $\omega_{LO} - \omega_{IF}$ , as expected from an upconversion, but it can also be appreciated that by choosing the values of  $I$ ,  $Q$ ,  $\phi_I$  and  $\phi_Q$  wisely we can make the signal of one of the two frequencies vanish, therefore yielding SSB upconversion. For example, we could use the right (upper) sideband by choosing  $I = Q$ ,  $\phi_I = 0$  and  $\phi_Q = 90^\circ$ , which would cancel the left (lower) sideband, therefore yielding the signal

$$s_{RF} = \frac{1}{2} \cos((\omega_{LO} + \omega_{IF})t). \quad (2.6)$$

To perform single sideband upconversion, we can use an IQ mixer together with another quadrature hybrid coupler, this time introduced in the IF port, as can be seen in figure 2.6. When using this system for upconversion, it will be equivalent to introducing in I and Q ports of the IQ mixer a signal (the IF) with same frequency and amplitude but with a phase difference of  $90^\circ$ . In this case, either the right or the left sideband is cancelled, therefore performing SSB upconversion.

### 2.3.3 Imperfections of IQ mixers

Aside from the general mixer imperfections which were discussed previously, IQ mixers display some additional imperfections which must be taken into account when working with them [7]. The main consequences of these imperfections will be a LO signal leakage in the output signal and a weak cancellation of the unwanted sideband.

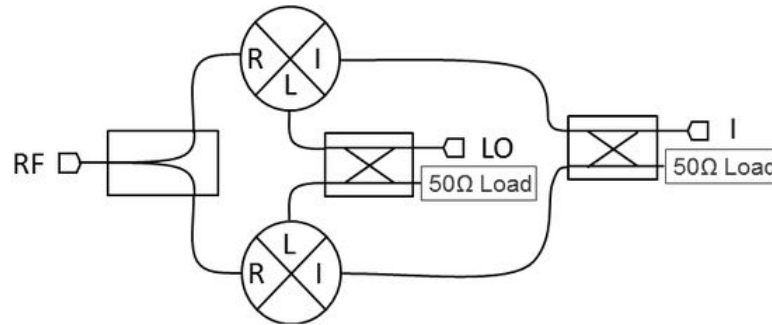


FIGURE 2.6: Internal structure of a single sideband mixer. Figure taken from [8].

One imperfection in IQ mixers is the DC-offset in both I and Q ports of the mixer. This offset is caused by a conversion loss imbalance between the two mixers which are inside the IQ mixer. The main consequence is that when performing upconversion with the IQ mixer a certain amount of the LO signal will leak in the mixer RF output. The LO to RF isolation, one of the metrics of an IQ mixer, quantifies this carrier leakage.

The other main imperfections found in IQ mixers are the amplitude and phase imbalances. Amplitude imbalances are caused by unbalances in the quadrature hybrid coupler and different conversion losses in each of the mixers. It means that the amplification/attenuation through the IQ mixer of each of the signals is not identical. The amplitude deviation of a mixer is the metric which quantifies the amplitude imbalance. On the other hand phase imbalances are due to phase unbalances of the hybrid coupler and different electrical connection lengths. This imbalance is indicated by the quadrature phase deviation of the mixer. Because of both of these imbalances the cancellation of the unwanted sideband will not be perfect.

For an optimal use of the IQ mixer for upconversion in our experiments, these imperfections are considered and minimized. To compensate the DC-offset in the IF, an external DC voltage input is applied in the I and Q ports in a way that the LO leakage is minimal. For the amplitude and phase imbalances, slight modifications in the amplitude and phase of the oscillating signal applied in Q are performed. These two schemes will yield an output signal with a single clear sideband signal, necessary for the experiments performed in the lab.

# Chapter 3

## Experimental procedure

In this chapter we will describe the structure and the different elements of the experimental setup and how are these configured to perform each of the different steps of the mixer calibration.

### 3.1 The experimental setup

To achieve the generation of microwave signals necessary to manipulate and do the read-out of the qubits, a system composed of diverse microwave instruments is required. The main components of this setup are the microwave signal generators (Rohde & Schwarz SMF100A), the arbitrary waveform generator (Tektronix AWG5014B), the frequency upconversion box and the frequency downconversion box.

The AWG generates the I and Q signals which will be upconverted by the IQ mixer in the upconversion box and afterwards sent to the sample for experiments or to the downconversion box for calibration. The microwave signal generators produce the LO signals necessary for the upconversion and the downconversion. All these different components of our setup are displayed in figure 3.2.

#### 3.1.1 The IQ microwave mixer

The mixer used in both the upconversion and the downconversion boxes of our setup is the IQ mixer IQ-0714 MXP from Marki microwave (figure 3.1). Its main metrics, all of which were defined in sections 2.2 and 2.3.3, are shown in table 3.1. The model of this IQ mixer is both used in the upconversion and the downconversion boxes, as this allows to work with the widest possible bandwidth. In the upconversion box it is used as an IQ mixer to perform single sideband and direct modulation, while in the downconversion box is just used as a regular three-port mixer by introducing a  $50 \Omega$  termination in one of the ports.

	IQ-0714 MXP
LO/RF frequency range	7-14 GHz
IF frequency range	DC to 500 MHz
Typical conversion loss	6.5 dB
Typical 1 dB compression point	6 dBm
Typical LO to RF isolation	25 dB
Typical quadrature phase deviation	3°
Typical amplitude deviation	0.4 dB

TABLE 3.1: Main metrics of the IQ mixer Marki IQ-0714 MXP.

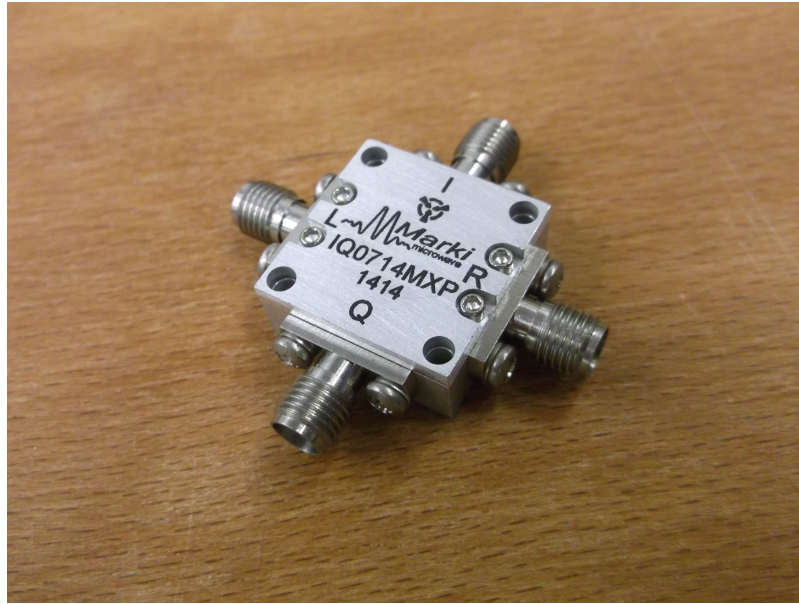


FIGURE 3.1: Marki IQ mixer IQ-0714 MXP.

### 3.1.2 The upconversion box

The upconversion box is the central component of the setup, as it is the part responsible of preparing the signal that will be later sent either to the sample in the cryostat or to the downconversion box to calibrate the IQ mixer.

It has three microwave signal inputs: the two intermediate frequency IQ signals coming from the AWG (frequencies not higher than 500 MHz) and the LO signal from a signal generator (frequency between 7-14 GHz). Before reaching the IQ mixer, both of the IF signals go through a 10 dB attenuator, which ensures that the power input in the mixer will not be higher than the 1 dB compression point (typically 6 dBm), as the maximum power that the AWG can supply is of 17 dBm. The LO signal is split by a power divider, half of the power going to the mixer and the other half going to a microwave switch which allows the signal to be sent to the sample for spectroscopy measurements.

The output of the upconversion box is handled by a microwave switch (SHX801-02-L-3-1-15 2P3T) with an external power supply of 24 V. This switch allows to either send to the sample the upconverted IQ signal generated from the AWG or the signal coming from the LO signal generator. Respectively, these two states of the switch also allow for

either sending no signal to the downconversion box or sending the upconverted signal to perform calibration of the IQ mixer.

### 3.1.3 The downconversion box

The downconversion box has two microwave inputs (the LO signal and the signal to be downconverted) and one single microwave output (downconverted signal). Together with the Analog-to-digital converter of the PCI it allows to perform a heterodyne measurement of the incoming signal. An additional microwave rotary switch (not represented in figure 3.2) allows to switch between different inputs to be downconverted, as for example the transmitted signal coming back from the sample. Since this thesis is focused only on the calibration scheme, the other possible inputs of the switch are not further discussed.

The IQ mixer in the downconversion box could also be used to perform homodyne detection, therefore allowing to measure a simultaneous read-out of the two quadratures. However, a  $50\ \Omega$  termination in the Q port of the mixer has been introduced in our setup, meaning that the mixer can be used as a regular three-port mixer and that the box is used for heterodyne detection. To be able to use the full range of the ADC, the output signal in the IF port of the mixer has to be amplified. Because of the fixed power output of the used amplifier (ZFL-500 LN), the signal must go through a 10 dB attenuator before being amplified. Two low-pass filters are also included before and after the amplifier to eliminate unwanted high-frequency signals and making sure that the output spectrum fits the ADC bandwidth.

Further experimental specifications of both the upconversion and downconversion boxes can be consulted in reference [9], in which technical features, losses of the different elements and states of the switches are described in detail.

### 3.1.4 Configuration of the AWG

The AWG is the instrument which will generate the relevant fields for both the DC-offset and the single sideband calibration. It has four different output channels, of which only two of them will be used, one for each quadrature component of the IF signal. Each one of these channels also has two marker outputs, of which we will use at least one to trigger the data acquisition in the PCI, while the others will only be used when pulse modulation of the signals is necessary, by gating the microwave signal generators.

On the other hand, the AWG can also provide a 4-channel DC voltage output, which in our setup has been connected to a voltage divider and then added to the channel inputs on the rear panel of the AWG. This DC output will be the one used for the DC-offset calibration.

To generate the desired fields or triggers in the AWG, it is necessary to create and load the patterns from the computer to the AWG hard drive. This is either manually done by generating the patterns with a *Mathematica* file and loading them from the AWG or automatically generated, stored and load by a *LabVIEW* program.



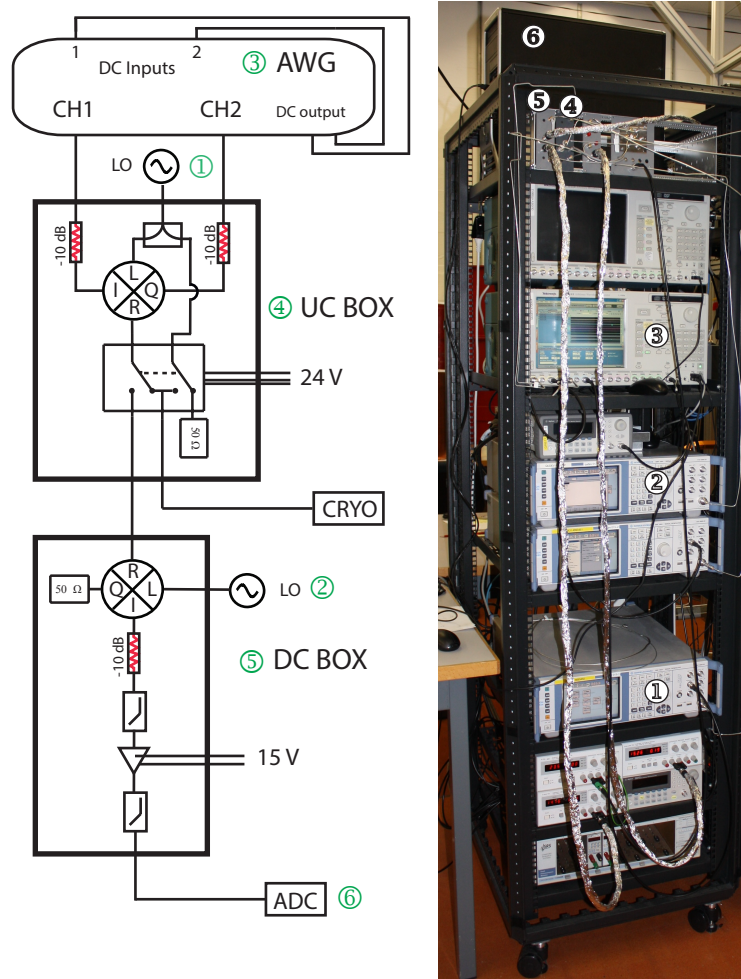


FIGURE 3.2: Experimental setup for the generation and measurement of the microwave signals.

## 3.2 IQ mixer calibration for continuous waves

The whole continuous wave calibration process of the mixer is automatized by the *LabVIEW* program *Mixer Calibration*. The program communicates through LAN/GPIB connection with the rest of microwave instruments to set the necessary configuration for the calibration and also retrieves the heterodyne measured data from the PCI.

### 3.2.1 DC-offset calibration

To perform the DC-offset calibration of the IQ mixer, the *Mixer Calibration* visual instrument mainly requires, aside from the details of the instruments used, the frequency of the desired LO signal as an input from the user. The program will set the indicated frequency in the microwave signal generator and prepare the patterns which will be sent to the AWG. Since this step of the calibration requires only of DC fields, all of the patterns will be a signal with zero amplitude, but with different DC outputs set. At each stage of the calibration process the program will sweep through different DC voltage steps for the I and Q ports and will measure the power of the output signal at the LO frequency, which will correspond to the LO leakage of the mixer. The program will

identify which DC values yield the minimal LO leakage and in the following stage will continue around these values with smaller steps. At the end of the calibration process, the best DC voltage values for the minimization of the leakage will be set in the AWG, in which new patterns can be loaded but keeping the DC output constant.

### 3.2.2 Sideband calibration

As explained in chapter 2, to compensate the amplitude and phase imbalances of the IQ mixer it is necessary to modify slightly the amplitude and phase of one of the quadrature IF signals to get a better cancellation of the unwanted sideband. In the *Mixer Calibration* program, the LO frequency, IF frequency, the IF amplitude and the desired sideband –right or left– must be indicated. With this information, the program will set the frequencies of the LO signal generators and this time it will generate sinusoidal patterns with the IF frequency indicated, and with fixed values of the amplitude and phase for the in-phase component but each of the patterns with slight phase and amplitude variations of the ideal case for SSB upconversion, e.g. same amplitude and  $90^\circ$  shift. This time the heterodyne measurement will be performed at the frequency of the unwanted sideband, and the program will search for the values which minimize the unwanted sideband power in a similar fashion to the DC-offset calibration process.

## 3.3 Pulsed direct modulation

The spur generation of higher harmonics, together with the LO leakage and the unwanted sideband signal, will affect the state of the qubit and the resonator in an uncontrolled way. This is particularly problematic for the study of geometric phases in superconducting qubits, as these states are specially sensitive to additional fields. Because of this we will proceed to perform direct modulation of the signal with a pulsed LO signal.

To modulate pulses at gigahertz frequencies it is necessary to apply an external gating pulse to the microwave signal generator. This pulse will be given by a marker output of the AWG, which because of the characteristics of the signal generator should not be shorter than 20 ns. The DC voltages applied in I and Q will also be pulsed with the same length as the gating pulse. Because of this, the patterns loaded in the AWG include both the signal of the LO pulse and the DC signals of the IF. These patterns are designed by a *Mathematica* file and loaded to the hard disk drive of the AWG. It is important to notice when creating the patterns that both the LO and the IF pulses should arrive to the mixer at the same time, which means that the different length of the coaxial cables as well as the delay time of the signal generator have to be taken into account. To do so, an oscilloscope allows to display the times at which the pulses reach the instrument, and by generating the gating pulse earlier in the AWG it is possible to synchronize the reception of the different pulses. This is described in figure 3.3 where the gating pulse (light blue) and the IF pulses (grey) are generated in the AWG, while the pulsed LO (oscillating pulse) comes from the microwave signal generator after the reception of the gating pulse. The delay between the pulses of 88 ns has been obtained from the measurements done with the oscilloscope.

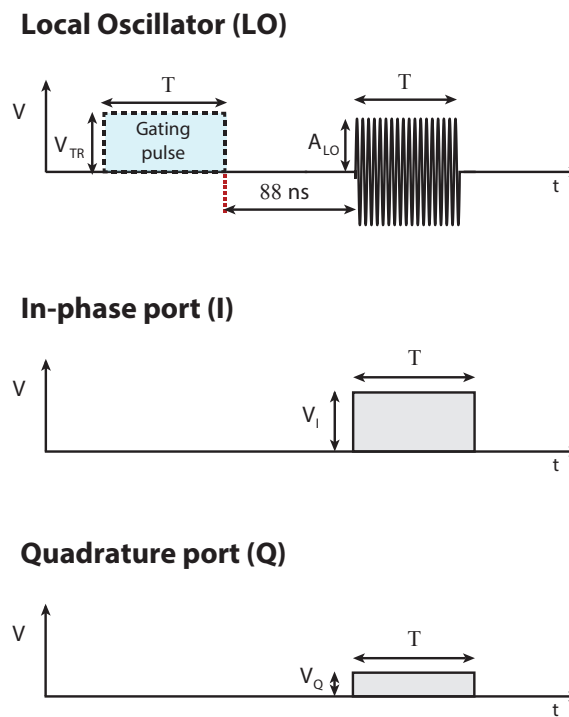


FIGURE 3.3: Graphical representation of the pulsing process of the LO and the IF DC voltages.

Once the calibration of the pulses generation times is done, pulses of different lengths can be generated ( $>20\text{ ns}$ ) and the phase of the output signal of the mixer can be modulated by modifying the amplitudes of the DC voltages in the I and Q ports.

## Chapter 4

# Results of the calibration

In this chapter, different measurements have been performed with the spectrum analyser to show some of the properties and imperfections discussed in chapter 2. On the one hand, spur generation and non-linearity are studied after continuous wave DC-offset and sideband calibration, while on the other hand the transmitted amplitude of pulsed signals from the mixer is measured for different phase modulations with and without DC-offset calibration.

### 4.1 Spectrum with continuous wave single sideband calibration

After proceeding with the offset and sideband calibration of the upconversion mixer by sending continuous waves, we can measure the spectrum of the output signal to study the behaviour of the LO leakage, the unwanted sideband and also the harmonics generated by the mixer. This is done by connecting the output of the upconversion box to a spectrum analyser connected by a GPIB cable to the computer and the rest of instruments. The data can be retrieved from a visual instrument of *LabVIEW*, which automatically changes the amplitude of the IF input power and sets the settings of the spectrum analyzer before extracting the spectrum data. The IF input power has been modified between 100 mVpp to 2 Vpp in steps of 100 mVpp, and this has been repeated for 5 different LO frequencies (7 GHz, 8.75 GHz, 10.5 GHz, 12.25 GHz, 14 GHz). The spectrum showed in figure 4.1 corresponds to a LO frequency of 7 GHz, an IF frequency of 0.1 GHz – this last frequency was the same for all measurements – and a sideband calibration performed at 400 mVpp of the IF input.

From the spectrum at low values of the IF input power, we can see that the main signal frequencies are  $f_{LO}$ ,  $f_{LO} + f_{IF}$  and  $f_{LO} - f_{IF}$ . These last two frequencies correspond to the two sidebands, where because of the calibration the lower one has been clearly cancelled and the upper represents the main carrier signal. However, as the IF input voltage grows to values higher than 1 Vpp, the generation of higher harmonic spurs clearly increases and up to 7 different frequencies can be seen in the spectrum.

By representing the power of each of the different harmonic signals, we can observe how the LO leakage and the unwanted harmonics evolve as the input power gets higher. This has been done in figure 4.2. To also quantify the power ratio between the different

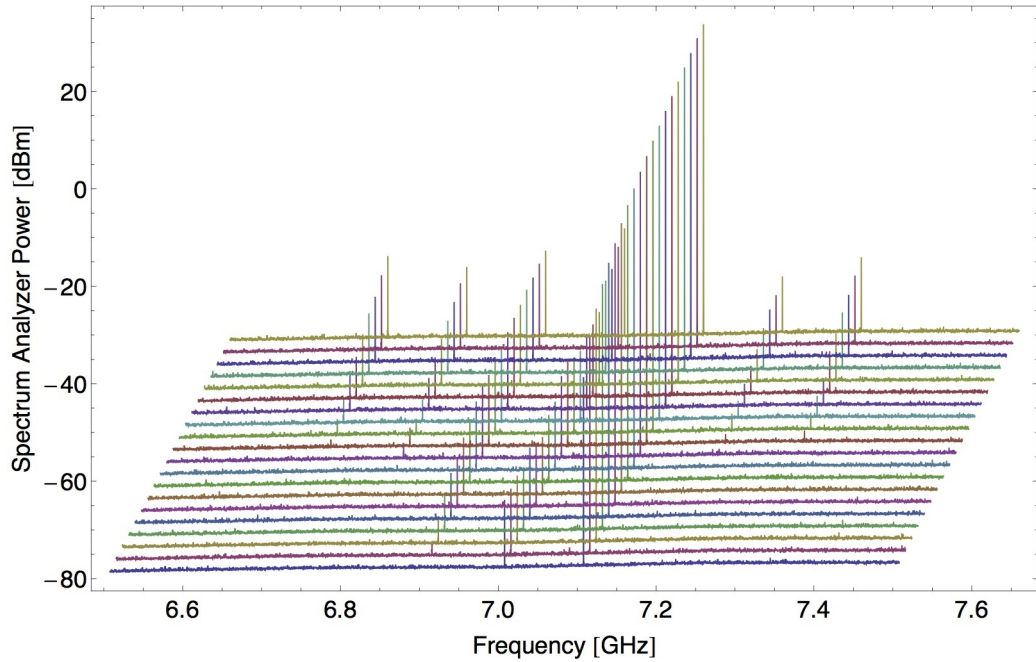


FIGURE 4.1: Spectrum after calibration for a  $f_{LO} = 7$  GHz,  $f_{IF} = 0.1$  GHz,  $V_{cal} = 400$  mVpp and AWG output voltage from 0.1 Vpp (closer to frequency axis) to 2 Vpp (further from frequency axis) in steps of 0.1 Vpp.

unwanted signals and the carrier signal, the power relative to the right sideband has been represented in dBc (decibels relative to the carrier) in figure 4.3.

## 4.2 Nonlinearity of the mixer

As it was described in section 2, when the power in the RF becomes too large, the output signal as a function of the input signal is no longer a linear function with slope 1. By representing the output power in the RF port of the right sideband as a function of the input power in the IF port, as in figure 2.4, we can identify at which input powers this nonlinearity starts to be present and avoid working with such high powers. In figure 4.4 we represent the points obtained by measuring the power of the right sideband obtained and by modifying the amplitude of the IF signal from 0.1 Vpp to 2.4 Vpp. To be able to appreciate correctly the effect of the nonlinearity, the voltages represented in the graphic correspond to the amplitude of the signals in the ports of the mixer, which have been calculated from the AWG output voltages and the spectrum analyser power by taking into account the losses in the attenuators, connectors and the other elements in the upconversion box.

To study the linearity of the mixer, a linear regression of the first nine data points has been computed and included in the graphic. The choice of taking only these points has been given by analysing the change of the R-squared parameter of the regression when including more or less of these points.

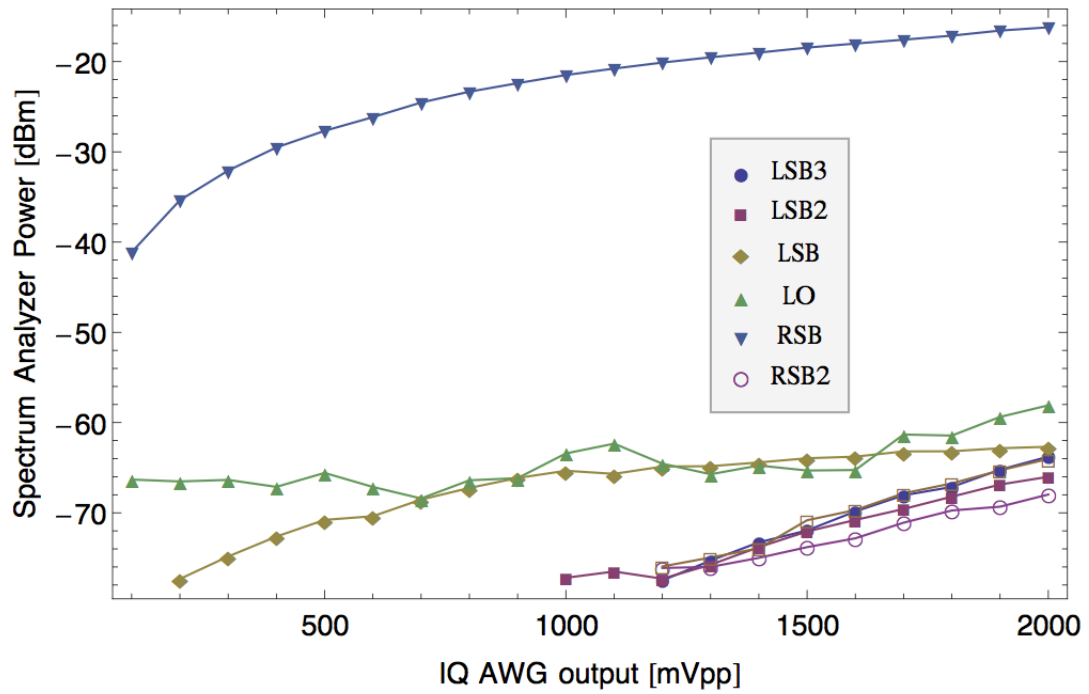


FIGURE 4.2: Power measured by the spectrum analyser at each of the different harmonic frequencies as a function of the AWG output voltage for a  $f_{LO} = 7$  GHz,  $f_{IF} = 0.1$  GHz,  $V_{cal} = 400$  mVpp.

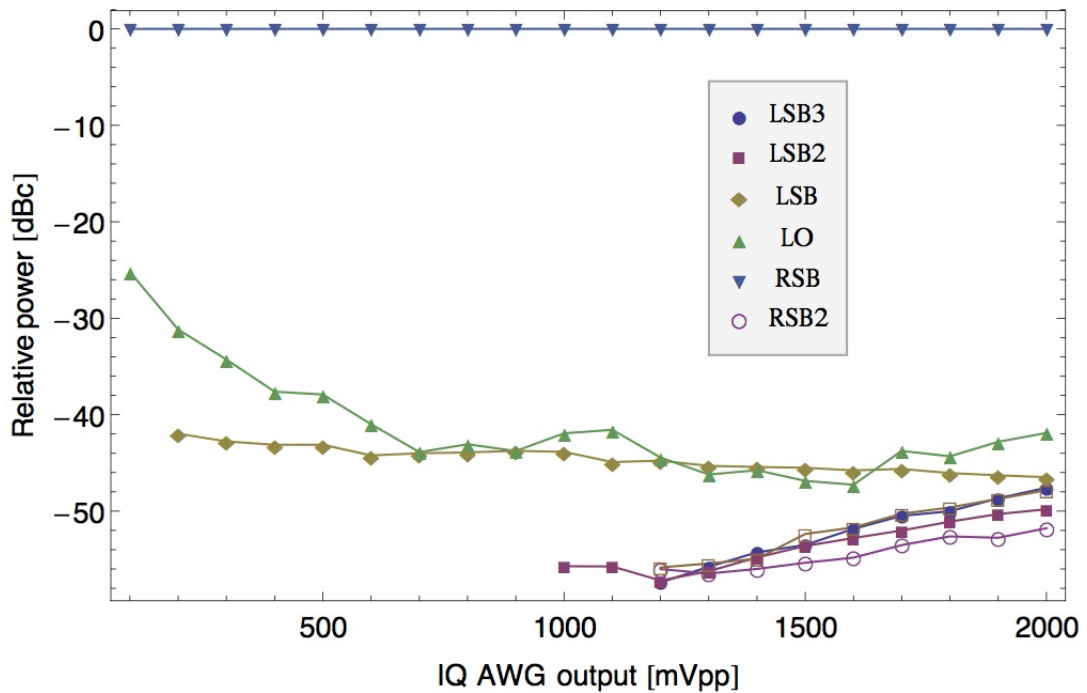


FIGURE 4.3: Power ratio to the carrier signal of each of the different harmonic frequencies as a function of the AWG output voltage for a  $f_{LO} = 7$  GHz,  $f_{IF} = 0.1$  GHz,  $V_{cal} = 400$  mVpp.

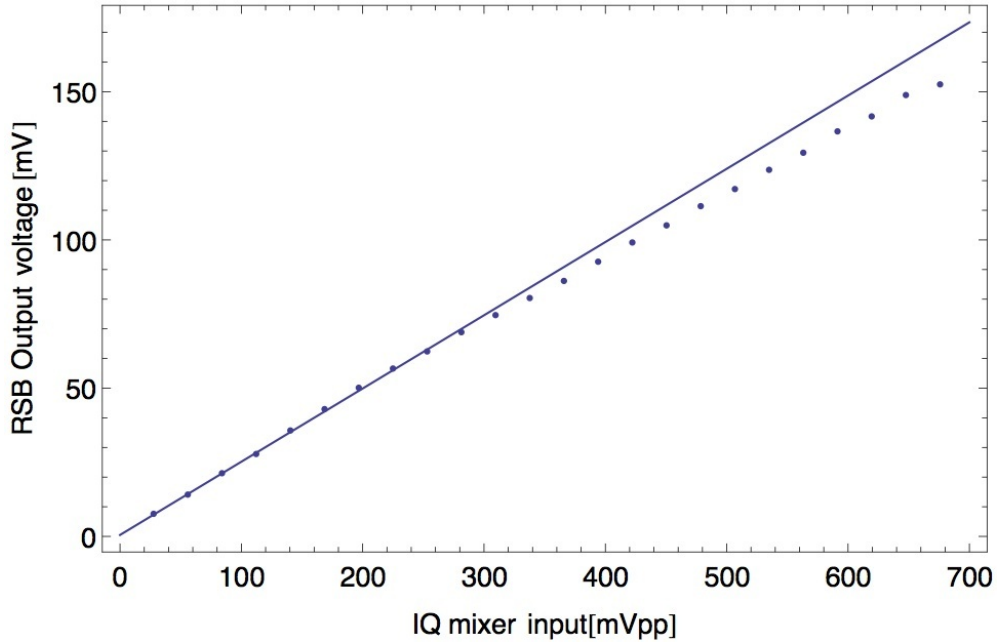


FIGURE 4.4: Output amplitude of the signal in the RF port as a function of the input voltage in the IF input for a  $f_{LO} = 7$  GHz,  $f_{IF} = 0.1$  GHz,  $V_{cal} = 400$  mVpp. A linear fit of the first nine points is also represented.

### 4.3 Direct pulsed modulation

With the procedure described in 3.3, we apply pulses of lengths from 20 ns to 2  $\mu$ s, and each pulse length is sent with 12 different phases, by modifying the amplitudes of the I and Q DC voltages. For each of these different pulse settings the output of the upconversion box is measured by the spectrum analyser. By computing the Fourier transform of a microwave pulse function we can understand the spectrum of such signal. If we model the pulsed signal as a sine with frequency  $\omega_{LO}$  multiplied by a square pulse of length  $\tau$ , we find that its Fourier transform is

$$|\hat{A}(\omega)| = \frac{\tau}{2\sqrt{2\pi}} \left[ \frac{\sin(\omega - \omega_{LO})}{\omega - \omega_{LO}} + \frac{\sin(\omega + \omega_{LO})}{\omega + \omega_{LO}} \right], \quad (4.1)$$

which can be seen as the sum of two sinc functions, one centered at the frequency  $\omega - \omega_{LO}$  and the other at  $\omega + \omega_{LO}$ . If  $\omega_{LO}$  is large compared with  $1/\tau$ , the second term is negligible for positives values of the frequency. Since the lowest frequency used with the mixer is of 7 GHz and the shortest pulse is of 20 ns, this approximation will always be valid for the results obtained. Since we now know that the signal measured by the spectrum analyser can be fitted with a sinc function centered at  $\omega_{LO}$ , we proceed to do so and take the amplitude of the fitted function for each of the pulses.

In figure 4.5 it can be seen how the measured spectra can be fitted by a sinc, though for higher values of the pulse, it is simpler to make the fit with a Lorentzian, as the sinc function approximates a Lorentzian as it gets narrower and higher. By fitting each of the measured spectra we can obtain the transmission peak at  $f = f_{LO}$  of each one of them, and represent the I/Q imbalance of the mixer for a given pulse length. To do so,

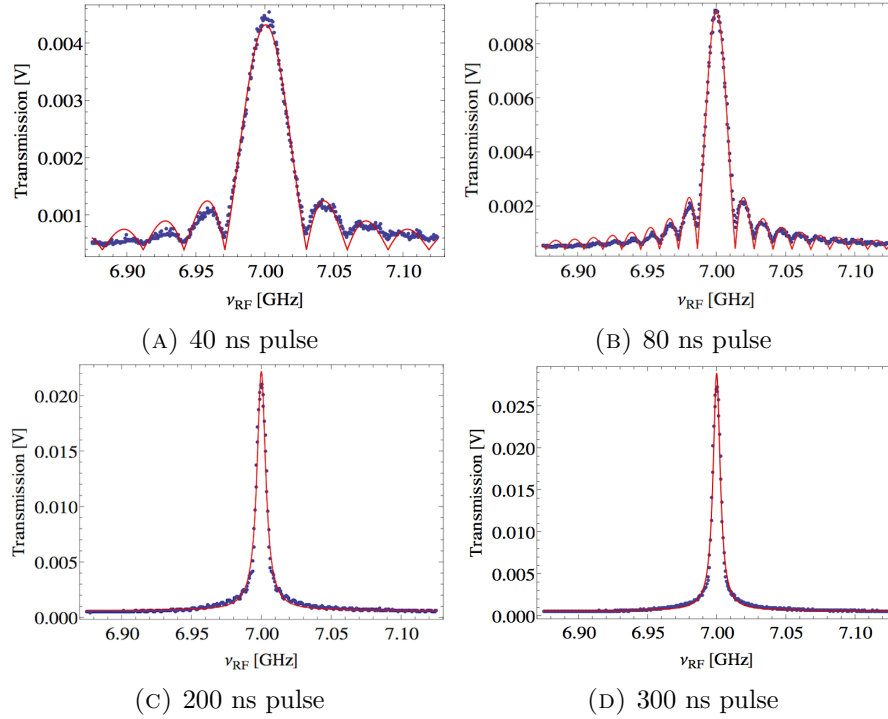


FIGURE 4.5: Transmission spectrum of the mixer measured for different pulse lengths

pulse length	DC-offset calibrated		Not calibrated	
	eccentricity	center distance	eccentricity	center distance
20 ns	0.37	0.02	0.28	0.06
60 ns	0.35	0.01	0.28	0.06
100 ns	0.35	0.02	0.29	0.06
140 ns	0.34	0.02	0.28	0.06
180 ns	0.35	0.02	0.26	0.06
220 ns	0.35	0.02	0.29	0.06
260 ns	0.34	0.02	0.27	0.06
300 ns	0.34	0.02	0.28	0.06

TABLE 4.1: Values of the eccentricity and center of the fitted ellipse obtained from points with different pulse lengths and either with or without performing DC-offset calibration.

we use an I/Q polar plot, where one point for each different phase is plotted. If we take each of the points as a phasor, they will have an angle  $\theta_i$  corresponding to the sent phase ( $\theta = \arctan\left(\frac{V_I}{V_Q}\right)$ ) and an amplitude  $R_i = V_i/V_1$ , which is basically the transmission normalized with one of the points. This representation allows to observe the phase imbalances, which can even be seen more clearly by fitting those points with an ellipse and using the eccentricity and the center of the ellipse as illustrative properties.

The shape of the imbalance does not change considerably when the length does. The results for pulses with lengths up to  $2 \mu\text{s}$  yield no difference in the imbalance shape. It can also be seen from the data of table 4.1, where the eccentricities and centers of the fitted ellipses are shown for some of the pulses, that with the calibration of the DC offset the center gets closer to the axis origin, though the eccentricity gets bigger.



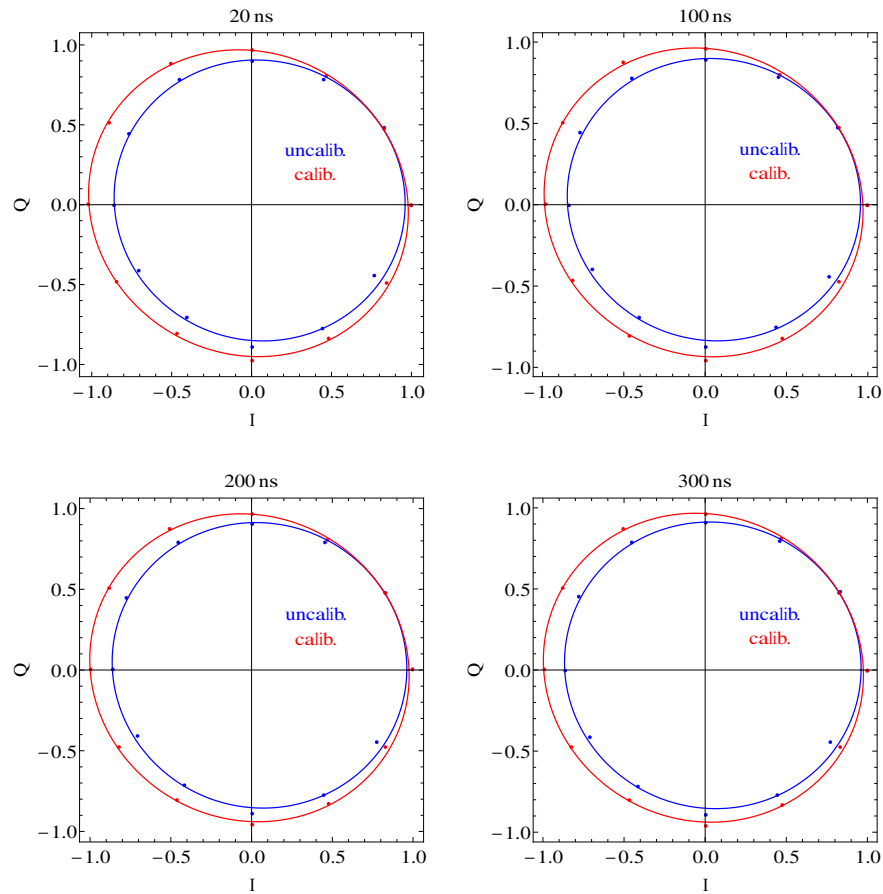


FIGURE 4.6: IQ transmission polar representation for different pulse lengths

Though the imbalance between I and Q –indicated by the eccentricity– cannot be solved by the DC-offset calibration, it can be taken into account when performing experiments by modifying the amplitude of the LO pulse according to the imbalance found during calibration, therefore yielding the same transmission for different values of the phase.

## Chapter 5

# Conclusions

The calibration of an IQ microwave mixer has been performed by using a routine which selects the values of the DC-offset at the IF ports which minimize the LO leakage to the RF port. This routine also allows to do single sideband modulation by sending microwave signals at the IF ports, and correcting the amplitude and phase imbalances of the mixer to maximize the suppression of the unwanted sideband. The suppression of both the LO leakage and the unwanted sideband has been measured, and how raising the input power modifies this suppression as well as generates additional harmonic spurs. Both the calibration and the spectrum measurements have been repeated with different frequencies of the LO signal (7-14 GHz), showing suppressions of the LO between -32 dBc and -44 dBc and cancellations of the LSB between -28 dBc to -45 dBc. The harmonic spurs reached power ratios of -45 dBc for the highest IF input powers. These same measurements have also shown the nonlinear behavior between the input and output powers of the mixer for high input powers, which increases the conversion loss of the mixer.

On the other hand, pulsed microwave fields were generated through direct modulation by pulsing the LO signal and the DC voltages applied in the IF ports. The transmitted signal was measured to represent the I/Q imbalance of the mixer when applying pulsed signals. The study of the imbalance for pulses with different lengths (20-300 ns) showed that its shape, characterized by the eccentricity of a fitted ellipse, did not change significantly. Because of this fact, the same amplitude calibration scheme can be used regardless of the length. As for the difference of these fits with and without the DC-offset calibration, the eccentricity was higher for the calibrated case but the center of the fitted ellipse was nearer the origin of the I/Q polar plot.

# Bibliography

- [1] D. P. DiVincenzo. The physical implementation of quantum computation. *Fortschritte der Phys.* **48**, 771, 2000.
- [2] A. Blais, R.-S. Huang, A. Wallraff, S. M. Girvin, and R. J. Schoelkopf. Cavity quantum electrodynamics for superconducting electrical circuits: An architecture for quantum computation. *Phys. Rev. A.* **69**, 062320, 2004.
- [3] A. Wallraff, D. I. Schuster, A. Blais, L. Frunzio, J. Majer, S. M. Girvin, and R. J. Schoelkopf. Approaching unit visibility for control of a superconducting qubit with dispersive readout. *Phys. Rev. Lett.* **95**, 060501, 2005.
- [4] R. Bianchetti, S. Filipp, M. Baur, J. M. Fink, M. Göppl, P. J. Leek, L. Steffen, A. Blais, and A. Wallraff. Dynamics of dispersive single-qubit readout in circuit quantum electrodynamics. *Phys. Rev. A.* **80**, 043840, 2009.
- [5] C. Marki F. Marki. Mixer basics primer. Technical report, Marki microwave, 2010.
- [6] S. Berger. Observation of a berry's phase in a transmon qubit. Master's thesis, ETH Zurich, 02 2010.
- [7] S. Sabah and R. Lorenz. Design and calibration of IQ-mixers. In *6th European Particle Accelerator Conference, Stockholm, Sweden*, 1998.
- [8] D. Jorgesen. Iq, image reject, and single-sideband mixers. Technical report, Marki microwave, 2013.
- [9] M. Fadel. Design and characterization of modular up and down converters. Technical report, ETH Zurich, September 2013.



Eidgenössische Technische Hochschule Zürich  
Swiss Federal Institute of Technology Zurich

## Declaration of originality

The signed declaration of originality is a component of every semester paper, Bachelor's thesis, Master's thesis and any other degree paper undertaken during the course of studies, including the respective electronic versions.

Lecturers may also require a declaration of originality for other written papers compiled for their courses.

---

I hereby confirm that I am the sole author of the written work here enclosed and that I have compiled it in my own words. Parts excepted are corrections of form and content by the supervisor.

**Title of work** (in block letters):

Calibration of an IQ mixer for continuous and pulsed modulation

**Authored by** (in block letters):

*For papers written by groups the names of all authors are required.*

**Name(s):**

Rubio Abadal

**First name(s):**

Antonio

With my signature I confirm that

- I have committed none of the forms of plagiarism described in the '[Citation etiquette](#)' information sheet.
- I have documented all methods, data and processes truthfully.
- I have not manipulated any data.
- I have mentioned all persons who were significant facilitators of the work.

I am aware that the work may be screened electronically for plagiarism.

**Place, date**

Zürich, 5th of August 2014

**Signature(s)**

*For papers written by groups the names of all authors are required. Their signatures collectively guarantee the entire content of the written paper.*